

# Realistic Physical Layer Modelling for Georouting Protocols in Wireless Ad-Hoc and Sensor Networks

Adnan Khan<sup>†</sup>, Costas Constantinou<sup>†</sup> and Ivan Stojmenovic<sup>‡</sup>

<sup>†</sup> School of Electronic, Electrical & Computer Engineering, University of Birmingham, Edgbaston, Birmingham, UK; email: {AXK353,c.constantinou}@bham.ac.uk

<sup>‡</sup> EET, FTN, University of Novi Sad, Serbia, and SITE, University of Ottawa, Canada; email: stojmenovic@gmail.com

## Abstract

*Existing routing and broadcasting protocols for ad-hoc networks assume an ideal physical layer. In reality, an accurate representation of physical layer is required for analysis and simulation of multi hop networking in sensor and ad-hoc networks. This paper describes the model for the lognormal correlated shadow fading loss from the first principles of probability theory, and investigates the importance of correlation length while designing protocols for ad-hoc and sensor networks. Nodes that are geographically proximate often experience similar environmental shadowing effects and can have correlated fading. We consider the overall path loss (shadow fading & median path loss) based on antennas working at 2.4 GHz with heights ranging from 0.5 metres to 1.8 metres. Finally, we analyze and compare the performance of localized position based greedy algorithm used for Unit Disk Graph (UDG) and probabilistic progress based algorithm on the proposed shadowing model for different values of standard deviation ( $\sigma$ ) of shadow fading to show the importance of both the shadow fading and correlation length.*

## 1. Introduction

Ad hoc networks have recently emerged as an important research topic, due to its potential application in various situations such as battlefield, emergency relief, environment monitoring etc [1-4]. They are decentralized, self-organizing wireless networks. Such networks consist of hosts that communicate without a fixed infrastructure. Communication takes place over a wireless channel. Since there is no infrastructure, every node has to determine its environment when the network is formed [5]. We assume that each node has a low-power Global Position System (GPS)<sup>1</sup> receiver, which provides the position information to the node itself

[5]. If GPS is not available then the distance between the nodes can be estimated on the basis of incoming signal strength [5]. In [6] it has been shown that relative coordinates of neighbouring nodes can be obtained by exchanging such information between nodes. The task of routing implies that a message has to be sent from a source node to a destination node.

Existing network layer protocols for ad-hoc networks assume an ideal physical layer model, where two nodes communicate, if and only if the distance between them is at most  $R$ . This model where the two nodes within transmission radius can exchange correctly bits, packets and messages is known as 'Unit Disk Graph' (UDG) model [5]. However, current physical layer models do not accurately represent radio channels in multi hop wireless networks [7], and as a result, there is a significant disconnect between simulation and real world deployment [8]. Channel models used in multi-hop networks have considered path losses to be independent, but they are correlated through shadowing effects [8]. The shadowing model is derived from the first principle of probability theory, which is then combined with the mean path loss model in [9] for low height antennas ranging from 0.5 metres to 1.8 metres working at 2.4 GHz to give an overall path loss model with correlated shadow fading. This shadowing model is then used for accurate representation of the physical layer, which is required for analysis, and simulation of multi-hop networking in sensor and ad-hoc network.

The next step is to compare and evaluate the performance of geographic routing algorithms over an ideal and a more realistic physical layer. For comparison purposes, localized position based greedy algorithms have been chosen where nodes do not require complete network topological information to perform the routing task. More precisely, nodes only require knowledge of the positions of itself, its one hop neighbours and the destination [5]. The ideal physical layer (UDG) uses a localized position based

greedy algorithm as proposed by Finn in [10], while the shadowing model considers the probabilistic progress based greedy algorithm that does not have hop-by-hop acknowledgements as in [11]. The ideal and the more realistic models are then evaluated in terms of average hop count (number of forwarding steps) over various average node densities, to show the dramatic difference of the two algorithms when using correlated shadow path loss model with different correlation lengths.

The rest of the paper is organized as follows. In Section-2, we present related work and offer some critical comments. In Section-3, we discuss the proposed correlated shadow-fading model with its derivation. Section-4 explains the overall path loss model for low height antennas used for 2.4 GHz range. Section-5 gives the background knowledge on the localized greedy algorithms. Section-6 discusses the measurement set up that is used to carry out the required experiment to compare the greedy algorithm used on UDG with the probabilistic progress algorithm used on shadowing model. Section-7 discusses the results that are obtained for average hop counts for the two algorithms (greedy and probabilistic progress) over range of node density. In Section-8, we provide concluding remarks and outline some open problems.

## 2. Related Work for Proposed Model

The long-term energy variability in multipath fading channels is widely accepted as being well described by lognormal statistics [12-14]. This phenomenon is commonly referred to as shadowing. While techniques such as power control may be successful in mitigating the effects of shadowing, an understanding of the phenomenon is important to a variety of techniques [15]. Not only shadowing but also its spatial correlation have been measured and shown to be significant in other wireless networks. For example in digital broadcasting, links between multiple broadcast antennas to a single receiver have correlated shadowing, which affects the coverage area and interference characteristics [17]. In cellular radio, the model of Gudmundson [18] is used to predict shadow correlation for the link between a mobile station (MS) to a base station over time as the mobile station moves. Gudmundson's model [18] is based on the assumption that the distance between the base station and mobile station is large compared to distance moved by the mobile. The reason why Gudmundson's model [18] is not appropriate to ad-hoc networks is because it can only be applied to pairs of links, which share a common node [8]. The other limitation is that it ignores the location of the common node [8].

The closest study which was useful in order to derive the shadow fading from first principles was presented in [8]. It studies the correlation of many disparate links at the same time, and uses multiple measured networks to examine many pairs of links with identical geometry, both with and without a common node. The other study, which was very useful in calculating the overall path loss model, is presented in [9]. This paper calculates the mean path loss model for low height antennas (0.5 metres to 1.8 metres) at 2.4 GHz, and it takes into account the effect of transmitter height, receiver height, receiver location and environmental parameters.

## 3. Correlated Shadow Fading Model with Derivation

In radio communications, the received signal level decreases as the distance between the transmitter and receiver increases. This phenomenon is described as 'pathloss' in [12,19]. Attenuation of radio signals due to pathloss effect has been modelled by averaging the measured signal powers over long times and over various locations with the same distance to transmitter [12]. The mean value of signal power is referred to as the area mean power.

The most commonly used radio model in ad-hoc networks is based on pathloss phenomenon alone and assumes that the received power at any distance to the transmitter is equal to the area mean power. If we assume that the transmitted signal is received correctly when the received signal power is more than a minimum required threshold value, this model result into a circular coverage area around the transmitting node (UDG). The area mean pathloss model is inaccurate because the received power level shows significant variations around the area mean power value due to the shadowing effect of terrain, height variation or the presence of mid-path obstacles [12]. In this paper we propose a more realistic radio model for the study of wireless ad-hoc networks. This model is based on the lognormal shadowing radio propagation model and allows for a spatially correlated random variation around the mean power. In lognormal radio model, the mean received power taken over all possible locations that are at a particular distance from the transmitter is equal to the area mean power calculated on the mean path loss model. However, it is further assumed that the average received power varies from location to location in an apparently random manner, which implies that variations in the path loss changes in a random manner as well. The standard deviation (SD) of fading is larger than zero, and in the case of severe signal fluctuations due to irregularities in the vicinity of the receiving and transmitting antennas, measurements indicate that it can be as high as 12dB.

For outdoor models, SD of correlated shadow fading can lie in the range of 6 to 12dB.

We start first from generating independent Gaussian random variables, using the Box-Muller method [20] in order to generate instances of a log-normally distributed random variable which describes shadow fading. There are a few methods to achieve this defined in [16], but the Box-Muller transformation method outlined in [20] is used in this paper.

Starting with two uniform deviates  $y_1$  and  $y_2$  on  $(0,1)$ , the transformation

$$\begin{aligned} x_1 &= \sqrt{-2 \ln y_1} \cos(2\pi y_2) \\ x_2 &= \sqrt{-2 \ln y_1} \sin(2\pi y_2) \end{aligned} \quad (1)$$

generates two Gaussian random deviates  $x_1$  and  $x_2$  with zero mean and unit variance, as can be seen from the Jacobian of the transformation,

$$\frac{\partial(y_1, y_2)}{\partial(x_1, x_2)} = \begin{vmatrix} \frac{\partial y_1}{\partial x_1} & \frac{\partial y_1}{\partial x_2} \\ \frac{\partial y_2}{\partial x_1} & \frac{\partial y_2}{\partial x_2} \end{vmatrix} = -\left(\frac{1}{\sqrt{2\pi}} \exp(-x_1^2/2)\right) \left(\frac{1}{\sqrt{2\pi}} \exp(-x_2^2/2)\right) \quad (2)$$

Scaling each of the Gaussian random deviates by the required variance  $\sigma^2$  results in the generation of a pair of independent Gaussian random variable instances,  $x'_1$  and  $x'_2$ , that can be used directly to model lognormal shadow fading,

$$\begin{aligned} x'_1 &= \sigma \cdot x_1 \\ x'_2 &= \sigma \cdot x_2 \end{aligned} \quad (3)$$

The next step is to produce a Gaussian random field and the two properties [23] play a very important role in it.

**Property 1:** For Gaussian processes, knowledge of the mean  $\mathbf{m}$  and the covariance  $\mathbf{C}$  provides a complete statistical description of the process.

**Property 2:** If the Gaussian process  $X(t)$  is passed through a linear, time-invariant system, the output of the system is also a Gaussian process, with a change in the mean value and the covariance of  $X(t)$ .

An important function, which could be derived from the covariance, is the correlation coefficient  $\rho$  [22].

$$\rho = \frac{\text{cov}(x_i, x_j)}{\sigma_i \sigma_j} = \frac{\langle (x_i - m_i)(x_j - m_j) \rangle}{\sqrt{\langle (x_i - m_i)^2 \rangle \langle (x_j - m_j)^2 \rangle}} \quad (4)$$

The correlation coefficient  $\rho$  is the range  $(-1, 1)$ . The covariance matrix  $\mathbf{C}$  for the multidimensional Gaussian process can be written in terms of  $\rho$  assuming that the two random variables have same standard deviation  $\sigma$  by using Equation (4) [23].

$$\mathbf{C} = \sigma^2 \begin{bmatrix} 1 & \rho_1 & \rho_2 & \dots & \rho_{n-1} \\ \rho_1 & 1 & \rho_1 & \dots & \rho_{n-2} \\ \rho_2 & \rho_1 & 1 & \dots & \rho_{n-3} \\ \vdots & \vdots & \vdots & \ddots & \vdots \\ \rho_{n-1} & \rho_{n-2} & \rho_{n-3} & \dots & 1 \end{bmatrix} = \sigma^2 P_n \quad (5)$$

The covariance matrix  $\mathbf{C}$  is called an ‘Autocovariance Matrix’ and the corresponding correlation matrix  $P_n$  is called an ‘Autocorrelation Matrix’. The values

inside the autocorrelation matrix can be replaced by the relevant autocorrelation function as shown in [9].

$$\rho_s(\Delta d) = \exp(-\Delta d/d_c) \quad (6)$$

The autocorrelation function is an isotropic correlation function. A stationary random field is an isotropic random field (in the wide sense) if the covariance function depends on the separation distance alone [24]. The significance of isotropic correlation functions is the simplicity as it only depends on the distance between the two points [24]. Using Cholesky’s algorithm for symmetric, positive definite matrices, the covariance matrix can be decomposed into a lower triangular matrix  $\mathbf{L}$  and an upper triangular matrix  $\mathbf{U}$  as explained in [20]:  $\mathbf{C} = \mathbf{L}\mathbf{U}$ , where  $\mathbf{U} = \mathbf{L}^T$ . (7)

$\mathbf{X}_s = \mathbf{L}\boldsymbol{\alpha}$  is a simulated random field (i.e. a  $n \times 1$  column vector of suitably correlated log-normal random variables on the constructed grid), where  $\boldsymbol{\alpha}$  consists of random, uncorrelated, univariate normally distributed random numbers  $\alpha_i$ ,  $i=1, \dots, n$  with zero mean and unit variance [20]. (8)

There are a few possible ways of choosing a grid to produce Gaussian field, for example in [24] a square grid and a few other geometrical shapes are chosen depending on the research criteria. The grid chosen in this paper is a circle with radius from 50 metres to 300m. In Figure 1, each circle in the grid is 50m apart, and each point on the same circle is 50m apart. The reason for choosing 50m apart is that if we choose the value of  $d_c = 70\text{m}$  and use Equation (6),  $\rho_s(\Delta d)$  is approximately 0.5. If the node which is used for the networking lies in the region of 4 grid points then the weighted average can be taken. The area between the four points can easily be found as every side is 50m apart which will help in interpolation rather than having irregular distribution of points. The angles from the inner most circle to the outer circles are 60, 30, 20, 15, 12 and 10 degrees, respectively.

#### 4. Overall Path Loss

The overall path loss in terms of distance can be calculated by adding the mean path loss between the transmitter and the receiver, the shadow fading loss and the loss from fast fading model, and is represented by (9) in logarithmic units [12].

$$PL(d) = L(d) + X_\sigma + 20 \log_{10} Y \quad (9)$$

$Y$  is random variable which describes the fast fading, and is neglected since we are considering the nodes to be static, (9) then reduces to:

$$PL(d) = L(d) + X_\sigma \quad (10)$$

$L(d)$  can be calculated from Konstantinou’s model for low height antennas as explained in [9], while  $X_\sigma$  is the element of  $\mathbf{X}_s$  corresponding to each grid location and can be calculated from Section-3,

and plotted in Figure-2.  $X_\sigma$  is a zero-mean Gaussian distributed random variable (in dB) with standard deviation also measured in dB. The lognormal distribution describes the random shadowing effects, which occur over a large number of measurement locations, which have the same transmitter–receiver separation, but have different levels of clutter on the propagation path. The LOS and NLOS equations, which were obtained by the least square criterion given by [9]:

$$PL_{LOS} = 4.62 + 20 \log_{10} \frac{4\pi}{\lambda} - 2.24h_t - 4.9h_r + 29.6 \log_{10} d \quad (11)$$

$$PL_{NLOS} = 20 \log_{10} \frac{4\pi}{\lambda} - 2h_r + 40 \log_{10} d + q \quad (12)$$

where  $\lambda$  is the free space wavelength,  $h_t$  and  $h_r$  are the transmitter and receiver heights above ground respectively, and  $q$  is an environment-dependent parameter given in [9].

If the terrain over which the path loss is modelled is not given then it is fairly difficult to use the Equations (11) and (12). Instead the probability  $\alpha$  that is the ratio of LOS and NLOS can be used to calculate the overall path loss given by [9]:

$$PL = \alpha PL_{LOS} + (1 - \alpha) PL_{NLOS} \quad (13).$$

(13) can be used for statistical treatment of path loss in typical urban environments. It approximates the LOS case in short distances, whereas it is practically the same with NLOS case at large distances from the transmitter. The probability  $\alpha$ , which does not depend on antenna height, is [9]:

$$\alpha(d) = \begin{cases} \exp\left\{-\frac{(d - a_f)}{b_f}\right\} & \text{if } d \geq a_f \\ 1 & \text{if } d < a_f \end{cases} \quad (14)$$

where  $a_f$  and  $b_f$  are environment-dependent (e.g. urban, suburban, open) threshold distances again given in [9].

## 5. Background Knowledge of Localized and Probabilistic Greedy Algorithm

In this section, we discuss the localized position based algorithms which have been used to compare the UDG model versus the model proposed in the above sections for low height antennas working at 2.4 GHz and having correlated shadow fading.

Localized *greedy* position based algorithm [10] is a well known greedy routing scheme, where the node currently holding the packet, will forward it to its one-hop neighbour which is closest to the destination. This algorithm fits well with the existing definition of transmission radius in Unit Disk Graph Model (UDG) [5]. All the nodes that lie within the transmission radius  $R$  of UDG are called ‘One Hop Neighbours’ to that particular node. The probability of packet reception, which is defined as the success of receiving a packet is 1 inside the transmission radius  $R$  while 0 outside it. The transmission radius of UDG is chosen

on the basis of IRIS mote receiver sensitivity and is found to be around 61 metres.

UDG model is not realistic because it ignores random variations in received signal strengths and was demonstrated to have a significant impact on ad-hoc network performance [11]. So UDG model will then be compared to the shadowing model, which shows the random variation in signal strength by correlated shadow fading model. The correlated shadow-fading model will use the *probabilistic progress* (PP) algorithm that does not have hop-by-hop acknowledgements. In PP algorithm, a node currently holding the message will forward it to one hop neighbour that maximises the expected progress, which is the product of the probability of packet successful reception (*ppr*) and the progress (difference in distance to destination of current and next node on the route) made by forwarding the packet to that node [11]. If we assume fixed signal to noise ratio (no shadow fading) then *ppr*, which depends on the distance, can be shown in Figure-3.

Packet reception probability (*ppr*), which is based on the calculation of bit error rate and packet length, is used to define one hop neighbours for the probabilistic progress algorithm. Two nodes are defined as neighbours if the *ppr* between them is above a certain minimum threshold [11] and for this study the transmission range  $R$  of the probabilistic progress algorithm scheme is chosen if  $ppr \geq 0.5$ . The two metrics that has been calculated on the UDG and shadowing model are the ‘network density’ and the ‘hop count’. Network density is defined as the average number of neighbours per each node that lies within the transmission radius of each node. Hop count is defined as the number of hops taken to reach from source to destination.

## 6. Numerical Experiment Set Up

We place  $n$  nodes in  $x \times x$  area, uniformly and randomly distributed. The  $x$  and  $n$  were varied to cover wide range of neighbouring node densities. We took the parameters of IRIS motes which work on 2.4 GHz and each node was assumed to have fixed transmitted power 3dBm (-27dBW) [26]. Channel parameters are assumed fixed during transmission of a single packet [27]. Quadrature Phase Shift Keying (QPSK) is assumed as the modulation scheme for communication system, which can be used to calculate *ppr*, for packet length 128 bits. Without using any forward error correction codes, *ppr* can be calculated by  $ppr = (1 - p_e)^L$ , where  $p_e$  is the bit-error-ratio (i.e. the probability of one bit being detected erroneously at the receiver) (15). Before running the greedy and the probabilistic progress algorithms, Dijkstra shortest path scheme was used to test the network connectivity and only connected graph were

used in measurements [5]. The proposed circular model as shown in Figure-1, which contains correlated shadow fading on all the points of the circular grid will be produced on every node in the area. Each node will be placed in the centre of the circular field and the correlated shadow fading can be produced as described in Section-3. Figure-4 shows how the circular proposed field has been plotted on the first few nodes.

## 7. Extended Simulation Results

Table 1 lists all parameters used in the simulation. The values 0, 6 and 8 dB for  $\sigma$ . The error bar graphs in Figures-6, 7 & 8 (which use different correlation lengths) show an average number of hops for particular densities. For collecting first set of results an area of 400m by 400m was chosen and the number of nodes used were 100, 125, 135, 150, 200, 250, 275 and 300. For the second set of results the area was increased to 500m by 500m and the number of nodes used were 250, 275, 300 and 325. In all simulations the node with the smallest x-axis coordinate is selected to be the source and the node with the largest x-axis coordinate is selected to be the destination.

### 7.1. Definition of Parameters

#### Parameter-1:- Correlation Length to UDG Transmission Radius Ratio

The correlation length is defined as correlation distance  $\Delta d$  in (6) that corresponds to a 50% correlation coefficient for the log-normal shadow fading spatial field. If the distance between the two receivers that are equidistant from a transmitting node is less than the correlation length, the power received by the two nodes will be similar. This argument implies that the ratio of correlation distance to an equivalent UDG transmission radius can be employed to characterise the angular separation of receivers at the edge of the reception area of a transmitting node, as seen at the transmitter. This ratio,  $\psi$ , will signify the importance of the correlation length of the proposed shadowing model.

$$\psi = \frac{\text{Shadow fading 50\% decorrelation dist}}{\text{Equivalent UDG Transmission Radius}} = \frac{d_{50\%}}{R} \quad (16)$$

We may define an equivalent UDG transmission range  $R$  by two methods, either by setting  $\sigma_{dB} = 0dB$  and taking  $ppr = 0.5$  as it will give a fully deterministic, circularly symmetric model for the probability of packet reception, or on the basis of the node receiver sensitivity where the transmission radius is calculated only on the basis of mean path loss (i.e.  $\sigma_{dB} = 0dB$ ). The parameter  $\psi$ , schematically shown in Figure-5 determines whether the correlated shadow fading  $ppr$  contour “amoeba” has many

protrusions/legs (low value of  $\psi$ ) or few such features (high value of  $\psi$ ).

#### Parameter-2: Standard Deviation of Shadow Fading

The standard deviation of shadow fading represented by  $\sigma$  is an important parameter as it measures the spread of the probability density function of the random variable and will help to increase the range of the shadow fading.

#### Parameter-3: - Network Density

The third parameter used for evaluation is the ‘Network Density’, which is defined as the average number of neighbours per each node that lies within the transmission radius of each node and is represented by  $\kappa$ . Varying the number of nodes and the size of the simulation area controls the average density.

$$\kappa = \frac{\text{Average number of neighbouring nodes (ppr} \geq 0.5)}{\text{Area of UDG}} \quad (17)$$

### 7.2. Interpretations of Plots for Extensive simulation

The greedy algorithm has a hop count close to the optimal (found by Dijkstra’s algorithm); local knowledge prevents it from finding always an optimal path, and sometimes it does not find a path at all in a connected network. When there is no shadow fading involved ( $\sigma = 0$ ), the transmission range which is still circular in this model was found to be approximately around 64 metres as shown in Figure-4, which is not much different from the transmission radius of UDG found by receiver sensitivity (61 metres) and that’s why the black line representing the probabilistic progress used for shadowing model with  $\sigma = 0$ , follows very closely to greedy algorithm on UDG. The performance of Dijkstra’s algorithm, the greedy algorithm applied on the UDG and the partially physically “realistic” model with no shadow fading  $\sigma_{dB} = 0$  dB can be seen to be comparable throughout in Figures-6, 7 & 8.

Average hop counts for  $\sigma = 6$  are shown by lime green colour in Figures-6, 7 & 8.  $\sigma = 6$  dB means that 99.7% of the shadow fading values produced on the circular field are within the range of +18 dB to -18 dB. At lower node densities ( $\kappa < 14$ ), the difference between the greedy on UDG and probabilistic progress algorithm with  $\sigma = 6$  dB is quite visible, while at higher node densities ( $\kappa > 18$ ), the average hop count is very similar. Probabilistic progress algorithm performs quite well on the shadowing model with shadow fading ( $\sigma = 6$  dB) for lower node densities. This is because PP may choose forwarding neighbor with  $ppr < 0.5$  while greedy algorithm may be left with neighbors with small progress (among those with  $ppr > 0.5$ ). For higher node densities, PP algorithm does not have the same advantage over

greedy on UDG hop count, for all the different values of  $\psi$ . The reason is that at higher node densities, the greedy on UDG will have more chance of utilizing its transmission radius of 61 metres. The shadowing model with  $\sigma = 8$  dB is represented by the colour magenta and has 99.7% of shadow fading in the range from +24dB to -24dB. The following observations have been made at different values of  $\psi$ :

1. When  $\psi = 1.63$  (Figure-6), due to higher standard deviation of shadow fading at  $\sigma = 8$  dB, the hop count of the PP on shadowing model is found to be approximately half the hop count on the same topology as compared to greedy on UDG. The correlated shadow fading with  $\sigma = 8$  dB contains more neighbouring nodes compared to the fixed neighbouring nodes in the case of greedy on UDG, and thus the hop count to destination is far less. The explanation of reduced hop count compared to greedy on UDG can also be related to the fact that the neighbours lying roughly along the preferred direction of message forwarding are effectively either “good” candidates for message forwarding or either they are all bad candidates, which depends on the produced shadow fading values. PP algorithm effectively favours forwarding nodes with predominantly “good” candidate neighbours, because the shadow correlation length of 100 metres is such that these clusters of neighbours sit over angular domains of the order of about one radian as seen by the forwarding node, which will result in choosing the next forwarding hop in the direction of destination. Since the next hop is chosen in the direction of destination then the hop count is reduced as compared to greedy on UDG and this advantage of the probabilistic progress algorithm is quite clear in Figure-7 for all node densities.

2. When the correlation length has been decreased to 30 metres ( $\psi = 0.49$  refer to Figure-7), probabilistic progress algorithm holds its advantage over UDG model at lower node densities in terms of hop counts. While at medium and higher node densities the values of average hop count are found to be very similar between the probabilistic progress algorithm using shadow fading and UDG model. Decreasing the correlation length means that the probability of having nodes with high values of  $ppr$  closest to the destination decreases. Since the correlation length has been decreased in length as compared to Figure-6, the probabilistic progress algorithm which chooses “good” candidates in the preferred direction of the destination will have higher hop counts because of the length of correlation, as the power received will not be dependent (correlated) between the two nodes beyond 30 metres, which will reduce the probability of finding clusters of neighbours sitting over angular domains of the order of about one radian as seen by

the forwarding node in comparison to the correlation length of 100 metres. Since the probability of having clusters of neighbours with the similar received power in the direction of destination is reduced therefore the hop count is increased as shown in Figure-7.

3. When the correlation length has been increased to 150 metres ( $\psi = 2.45$  refer to Figure-8), PP algorithm again holds its advantage over greedy on UDG model at lower node densities ( $\kappa$ ), in terms of hop counts. At medium and higher node densities the values of average hop count for PP and greedy algorithms are found to be very similar. Since the correlation length has been increased in length as compared to Figure-6 (100 metres), PP algorithm which chooses “good” candidates in the preferred direction of the destination will have higher hop counts because of the correlation function which is an exponential function and the power received will decrease between the two nodes exponentially as the distance between the two nodes increases, which will reduce the probability of finding neighbours with high values of metric ( $ppr \times \text{progress made}$ ) at larger distances over angular domains of the order of about one radian as seen by the forwarding node in comparison to correlation length of 100 metres.

## 8. Conclusion

In this work we have shown that a meaningful assessment of a geographic, position-based routing protocol can only be achieved through careful incorporation of the physics of radiowave propagation in simulations. We demonstrate that UDG based models, and models that fail to take into account the fully correlated spatial distribution of link reliability, significantly over-predict the end-to-end path hop count. The only geographic routing algorithm that has been found to be capable of exploiting the distant neighbour forwarding opportunities that occur in physically realistic radiowave propagation environments, and thus exploited end-to-end paths requiring fewer hops, is the localised probabilistic progress algorithm [11]. In [11] it was derived, analytically and experimentally, that the expected hop count (where the expected number of retransmissions per hop are  $1/pr$ ) for PP algorithm is superior to the one offered by greedy algorithm (applied as in this article). This article makes a step further, to show that, surprisingly, even simple hop count of PP can be superior to the one of the greedy algorithm. The simplification of using hop count rather than expected hop count can only favour the greedy algorithm if PP chooses consistently hops of low  $ppr \ll 0.5$ , which is an impossibility given that the next hop selection algorithm for PP is based

on maximising the  $ppr \times$  progress criterion amongst candidate next-hop neighbouring nodes.

We have provided a complete overview of the manner in which the physical radio environment needs to be modelled. Furthermore, we have identified three parameters that are required in order to meaningfully characterise position-based routing and provided a geometric interpretation for these:

- The angular spread of regions of higher than average range for a given probability of packet reception,  $\psi$ , which is determined by the shadow fading de-correlation length and the notional node transmission radius,
- The extent to which such regions are pronounced, given by the shadowing standard deviation  $\sigma_{dB}$ , and
- The average local node density,  $\kappa$ , which ultimately determines the probability with which such regions are populated by neighbouring nodes.

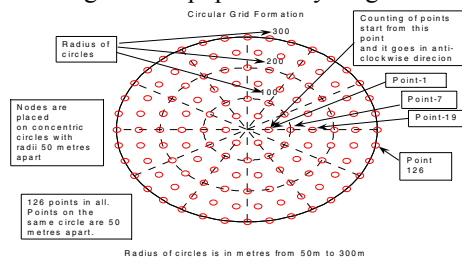


Figure-1: - Circular Grid Plot

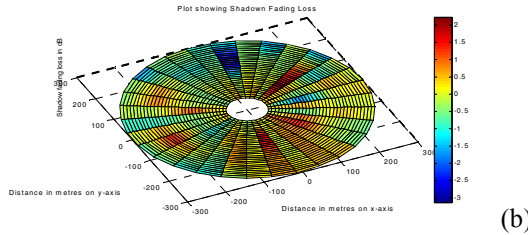
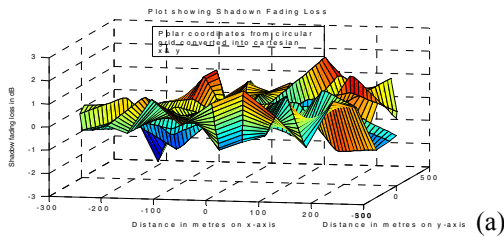


Figure-2: - Polar plot representation for shadow fading losses in circular field  
Note: - For further detail about this plot consult [26]

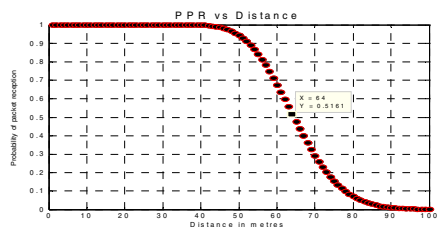


Figure-3: Probability of Packet Reception vs Distance

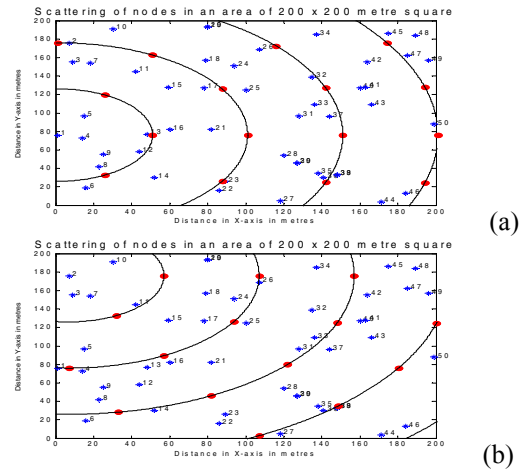


Figure-4: - Shadow fading circular model on first four nodes in an area of 200 by 200 metre square; (a) node-1 as centre (b) node-2 as centre

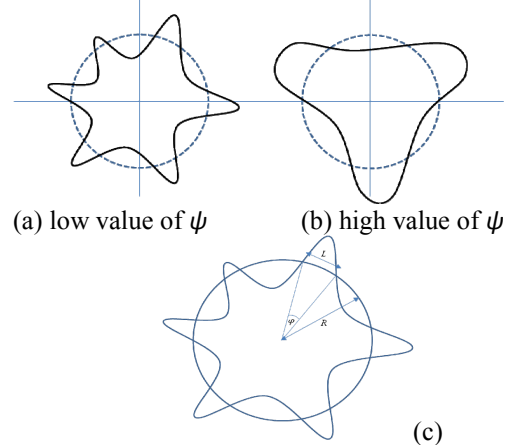


Figure 5: Typical  $ppr$  contours (solid lines)  
(a) a low value of  $\psi < 1$ , (b) a high value of  $\psi > 1$ ; (c) For  $\psi \leq 1$ , the ratio  $\psi$  is approximately equal to the angle in radians, as observed at the transmitting node, where  $d > d_{50\%} = R = 70m$  for its  $ppr = 0.5$  contour, since (maximum error of 4%)  
 $\psi = L/R = 2 \sin \frac{1}{2} \phi \approx \phi$  for  $\phi \leq 1^c$ .

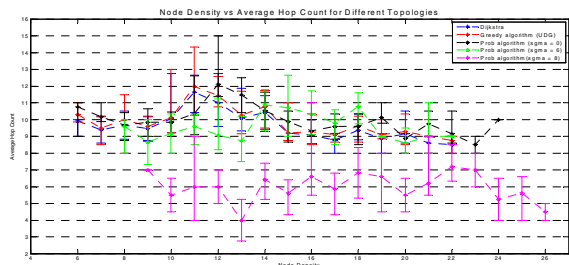


Figure-6: - Average Hop Count vs Node density of Dijkstra, greedy on UDG and Probabilistic progress on realistic physical layer with correlation length of 100 metres ( $\psi = 1.63$ )

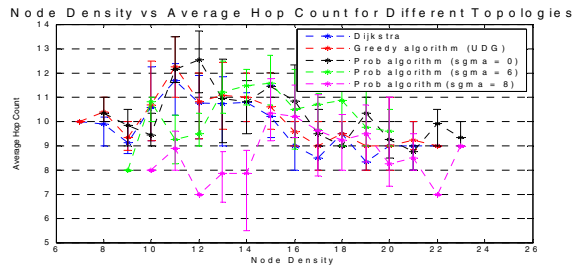


Figure-7: Ibid, correlation length 30m ( $\psi = 0.49$ )

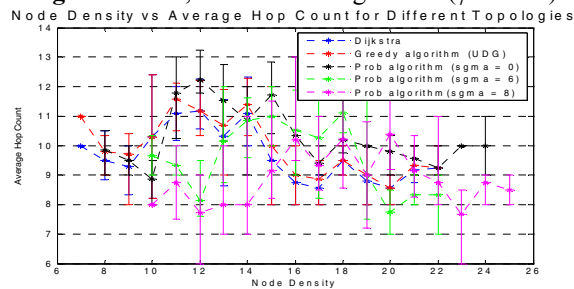


Figure-8: Ibid, correlation length 150m ( $\psi = 2.45$ )

PARAMETERS USED IN SIMULATION	
Height of Transmitter Antenna	1.5 m
Height of Receiver Antenna	1.5 m
Power Transmitted from Transmitter	-27dBW
Receiver Sensitivity	-131dBW
Packet Length	128 bits
Threshold for Probabilistic Greedy Algorithm	0.5
Degree of Reed Muller Coding	3
Path Loss Exponent	4

Table-1: - Parameters For Extensive Simulation

## 9. References

[1] S. Basagni, M. Conti, S. Giordano, I. Stojmenovic (eds.), "Mobile Ad-Hoc Networking," IEEE Wiley, 2004.

[2] M. Kahn, R. H. Katz, and K. S. J. Pister, "Next century challenges: Mobile networking for "smart dust"," in *International Conference on Mobile Computing and Networking (MOBICOM)*, 1999, pp. 271-278.

[3] S. Giordano, "Mobile Ad Hoc Networks," in *Handbook of Wireless Network and Mobile Computing*, I. Stojmenovic (ed.), Wiley, 2002, pp. 325-346.

[4] G.J. Pottie and W.J. Kaiser, "Wireless integrated network sensors," *Communications of the ACM*, vol. 43, no. 5, pp. 551-558, 2000.

[5] Kuruvila J., Nayak A., Stojmenovic I., Hop count optimal position based packet routing algorithms for ad hoc wireless networks with a realistic physical layer; *IEEE Journal of Selected Areas in Communications*, Vol. 23, No. 6, 2005, Pages 1267-1275.

[6] D. Niculescu, "Positioning in ad hoc sensor network," *IEEE Network*, July 2004, Pages 24-29.

[7] H. Lee, A. Cerpa, and P. Levis, "Improving wireless simulation through noise modeling," in *Information Processing in Sensor Networks (IPSN'07)*, April 2007.

[8] Agrawal, Piyush, and Patwari, Neal, Correlated Link Shadow Fading in Multi-hop Wireless Networks; Dept. Electrical and Computer Engineering, University of Utah, Salt Lake City, USA, manuscript, 2008.

[9] K. Konstantinou, S. Kang and C. Tzaras, "A Measurement-Based Model for Mobile-to-Mobile UMTS Links," *IEEE 65th VTC*, Spring-2007, pp. 529-533.

[10] Finn G. G., Routing and Addressing Problems in Large Metropolitan-Scale Internetworks, ISI res. rep. ISU/RR- 87-180, 1987.

[11] Stojmenovic, I., Nayak, A., Kuruvila, J., Design Guidelines For Routing Protocols In Ad hoc And Sensor Networks With A Realistic Physical Layer; *IEEE Communication Magazine*, 43, 3, March 2005, 101-106.

[12] W. C. Jakes, Ed., *Microwave Mobile Communications*. Piscataway, NJ; IEEE Press, 1994.

[13] G. L. Turin, F. D. Clapp, T. L. Johnston, S. B. Fine, and D. Lavry, "A statistical model of urban multipath propagation," *IEEE Trans. Veh. Technol.*, vol. VT-21, pp. 1-9, Feb. 1972.

[14] F. Hansen and F. I. Meno, "Mobile fading—Rayleigh and lognormal superimposed," *IEEE Trans. Veh. Technol.*, vol. VT-26, pp. 332-335, Nov. 1977.

[15] C. Chysanthou and H. L. Bertoni, "Variability of sector averaged signals for UHF propagation in cities," *IEEE Trans. Veh. Technol.*, 39, pp. 352-358, Nov. 1990.

[16] A. Papoulis, *Probability, Random Variables, and Stochastic Processes*. New York: McGraw-Hill, 1965.

[17] G. Malmgren, "On the performance of single frequency networks in correlated shadow fading," *IEEE Trans. Broadcasting*, 43, no. 2, pp. 155-165, June 1997.

[18] M. Gudmundson, "Correlation model for shadow fading in mobile radio systems," *IEEE Electronics Letters*, vol. 27, no. 23, pp. 2145-2146, November 1991.

[19] Hekmat, R ; Mieghem, P. Van, Connectivity in wireless ad-hoc networks with a log-normal radio model; Delft Univ. Technology, El. Engineering, Mathematics and Computer Science, The Netherlands, 2006.

[20] William H.; Teukolsky, Saul A.; Vetterliog, William T.; Flannery, Brian P., *Numerical Recipes: the art of scientific computing*, Cambridge University Press, 2007.

[21] John G.Proakis; Masoud Salehi, *Contemporary Communication System using Matlab*, 1999).

[22] Stremmler, Ferel, *Introduction to Communication System*, Third edition; Reading, Addison-Wesley 1990.

[23] George EP Box, Gwylin M Jenkins, Gregory C Rensil, *Time Series Analysis, Forecasting and Control*, Third edition; John Wiley & Sons Inc., 1994.

[24] Abrahamsen, Peter, *A review of Gaussian Random fields and correlation functions*, 1997, Second edition.

[25] [www.mathworks.com/matlabcentral/fileexchange/7656](http://www.mathworks.com/matlabcentral/fileexchange/7656)

[26] [www.xbow.com/Products/Product\\_pdf\\_files/Wireless\\_pdf/IRIS\\_Datasheet.pdf](http://www.xbow.com/Products/Product_pdf_files/Wireless_pdf/IRIS_Datasheet.pdf)

[27] Li C.P., Hsu W.J., Krishnamachari B., Helmy A., A local metric for geographic routing with power control in wireless networks, *IEEE SECON*, 2005.